


Coordinated reactive power and crow bar control for DFIG-based wind turbines for power oscillation damping

Wind Engineering
1–19
© The Author(s) 2018
Reprints and permissions:
sagepub.co.uk/journalsPermissions.nav
DOI: 10.1177/0309524X18780385
journals.sagepub.com/home/wie


Likin Simon¹ , Jayashri Ravishankar² and K Shanti Swarup¹

Abstract

The fault ride through capability and fast controller action makes doubly fed induction generator based wind energy conversion system to actively participate in power oscillation damping. This article describes a coordinated reactive power control from grid side converter along with active crowbar scheme for doubly fed induction generator which can actively participate in power oscillation damping, and thus improve the transient stability margin of entire power system. For a reactive power oscillation damping (ΔQ power oscillation damping), it is essential that the phase of the modulated output is tightly controlled to achieve a positive damping. Detailed 3 generator 9 bus Western System Coordinating Council system is modeled in PSCAD/EMTDC with the generator dynamics. The dynamics in power flows generator rotor speeds and voltages are analyzed followed by a three-phase fault in the power system. A set of comprehensive case studies are performed to verify the proposed control scheme.

Keywords

Crow bar doubly fed induction generator, oscillation, power oscillation damping controller, reactive power, wind energy conversion systems

Introduction

The widespread use of renewable energy generation in power industry makes the power system's control and operations more complicated and intrinsic. The intermittent and unpredictable nature of power output from the renewable sources increases the complexity of power system computations. Because of a non-polluting nature and economic viability, wind energy conversion system (WECS) becomes the most popular renewable energy source.

Doubly fed induction generator (DFIG)-based WECS became most popular among wind energy sources because of its high energy transfer capability (Miller, 2010), variable wind speed operation (Akhmatov, 2002) and maximum power extraction from the wind turbine (Shen et al. 2009). The independent active and reactive power control and four quadrant operation makes DFIG-based WECS unique in the renewable energy sector (Datta and Ranganathan, 1999; Xu and Cheng, 1995).

A DFIG-based WECS primarily consists of three parts: wind turbine drive train, a doubly fed induction machine and back-to-back converter as shown in Figure 1. Wind drive train consists of turbine which extracts mechanical wind energy, gear box which converts the shaft speed acceptable to the induction machine and the associated control system like pitch and stall controls to regulate the wind power (Pena et al., 1996). The back-to-back voltage source converter (VSC) is capable of bidirectional power flow irrespective of wind speed.

The fault ride through (FRT) capability of DFIG makes it possible to stay connected to the grid during the disturbance and maintain synchronism after clearing the fault (Ling, 2016) in the power system. The literatures have proposed the use of static var compensator (SVC) and STATCOM to improve the system inertia (Molinas et al., 2008). But the rating of the SVC and STATCOM need to be improved for an acceptable transient stability margin. To have a reasonable stability margin, the rating should be as good as that of WECS, which increases the overall cost and complexity of the system.

¹Department of Electrical Engineering, Indian Institute of Technology Madras, Chennai, India

²School of Electrical Engineering and Telecommunications, University of New South Wales Sydney, Sydney, NSW, Australia

Corresponding author:

K Shanti Swarup, Department of Electrical Engineering, Indian Institute of Technology Madras, Chennai, India.
Email: swarup@ee.iitm.ac.in

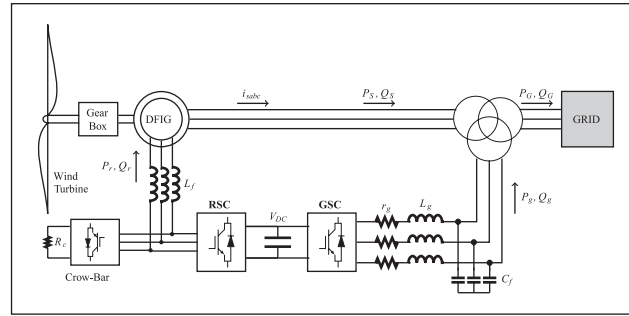


Figure 1. Configuration of DFIG.

The impact of increased penetration of DFIG-based wind turbine generators on transient stability of the system is discussed in the study by Hossain (2017). The change in dynamics and operational characteristics of the conventional grid due to the large penetration of DFIG is addressed. A decoupled FRT technique to enhance the system stability is discussed in the study by Meegahapola et al. (2010). The optimal crowbar resistance is found to improve the power transfer capability of the system. But the crow bar remains inactive once the fault is isolated from the system.

A method to improve the stability of offshore wind farm by the control of static series compensator in the transmission is discussed in the study by Wang and Vo (2013). Frequency domain analysis using the eigenvalue is discussed. The pole placement method using modal control theory is used for damping control. The inherent nature of DFIG rotor oscillations damping for local mode of oscillations is not discussed in detail. The study by Singh et al. (2015) proposes a control strategy to damp the inter area power oscillations by injecting the active power into the system out of phase with the potentially unstable mode.

Hughes et al. (2006) proposed a power system stabilizer (PSS) for DFIG-based WECS. The oscillation damping is obtained by controlling the DFIG terminal voltage magnitude and phase angle as conventional PSS works in synchronous machines. The stability study of power system with WECS, the nature of power oscillations in the system and rotor angle dynamics are discussed in the studies by Poller (2003) and Muljadi et al. (2007). These PSS would be designed to damp out specific frequency oscillations which may not be the same for all disturbances. The power oscillations after the fault clearance will have a variable frequency which depends on the distance of fault from the machine, fault impedance and stiffness of the grid. Normally, the frequency of oscillation is in the range of 0.2–12 Hz. The performance analysis of unified DFIG with dedicated controllers during fault and reactive power support is discussed in Rajpurohit and Singh (2015) and Gupta et al. (2017). These papers do not account for any coordination with reactive power modulation.

Edrah et al. (2016) discuss the effect of replacing all the conventional synchronous generators PSS with DFIG PSS. Reactive power modulation incorporating stochastic nature of wind speed is discussed. But crowbar remains disconnected once the fault is cleared. In Geng et al. (2017), a hybrid modulated active power modulation technique is proposed. The frequency response method discussed in the paper cannot address the coordinated action with reactive power modulation which have a direct affect on voltage magnitude.

The fast controller action of DFIG provides a dynamic control of reactive power support to the grid along with active crowbar switching. This article proposes a method to modulate the DFIG reactive power supply from the grid side converter (GSC) in coordination with active crowbar control to damp out the power oscillation in the system. This study shows, the location of fault have direct affect on reactive power modulation for power oscillation damping. The advantage of the proposed control scheme is that no dedicated communication devices or any other additional hardware equipments are required for the control. The control schemes associated with the back-to-back converters and crowbar converter is slightly rearranged in such a way that a compensating electromagnetic torque is developed in the machine to damp out the power oscillations. Section “Transient model of DFIG” describes the transient modeling of induction machine with stator flux oriented reference frame. Transient simulation modeling of Western System Coordinating Council (WSCC) system is described in section “Modeling of Power System” followed by the proposed reactive power control of DFIG in “Power Oscillation Control.” Various cases are simulated in PSCAD/EMTDC to verify the proposed control by applying the fault at different buses in section “Simulation Results.”

Transient model of DFIG

The basic circuit configuration of DFIG is as shown in Figure 1. The stator terminal of wound rotor induction machine is connected to the grid and rotor terminals through a step up transformer to reduce the voltage rating of the converters.

During different mode of operations like sub synchronous and super synchronous, the rotor circuit needs to supply power in both directions (Simon and Swarup, 2016). The back-to-back converters of insulated-gate bipolar transistor (IGBT) switches with anti parallel diodes are employed as shown in Figure 1 which allows the bidirectional power flow. The DFIG is modeled in synchronous reference frame (d - q) for the independent control of active and reactive power (Hassan et al., 2011; Muller et al., 2002).

RSC control

For rotor side converter (RSC) control, synchronous reference frame d axis is aligned with the stator flux of the machine for independent active and reactive power control of DFIG. The main objective of RSC is to control the excitation current of the machine and to operate the machine at desired rotor speed. The reference rotor speed will be corresponding to the maximum power tracking speed from the turbine torque speed characteristics (Shen et al., 2009).

The electromagnetic torque developed in the machine can be expressed in terms of direct and quadrature axis currents and flux as follows

$$T_{em} = \frac{3}{2} P \frac{L_m}{L_s} (\psi_{qs} i_{dr} - \psi_{ds} i_{qr}) \quad (1)$$

where T_{em} is the electromagnetic torque developed, P is the number of poles, L_m and L_s are the mutual and self inductances of the machine, respectively; ψ_{ds} and ψ_{qs} are d axis and q axis stator fluxes; and i_{dr} and i_{qr} are d axis and q axis rotor currents.

The synchronous rotating frame is selected as d axis and is aligned with the stator flux which results in

$$\psi_{ds} = \psi \text{ and } \psi_{qs} = 0 \quad (2)$$

Then the torque equation reduces to

$$\psi_{ds} = \psi \text{ and } \psi_{qs} = 0 \quad (3)$$

Similarly

$$\psi_{ds} = \psi \text{ and } \psi_{qs} = 0 \quad (4)$$

where i_{ms} is the magnetizing current; σ_s is the stator leakage factor, $\sigma_s = \frac{L_s}{L_m}$; i_{sd} and i_{sq} : d axis and q axis stator currents.

Therefore, the reactive power required to provide the magnetizing current can be fed either from stator side or rotor side. In this article, all the magnetizing current is fed from rotor side to maintain unity power factor at the DFIG terminals. The torque/rotor speed can be regulated by controlling i_{qr} and magnetizing current by i_{dr} .

Figure 2 shows the method to extract the stator flux from the stator voltage and currents. The stator side voltage balance equation can be written as

$$V_s = R_s i_s + \frac{d\psi_s}{dt} \quad (5)$$

Therefore, the machine flux can be written as

$$\psi_s = \int (V_s - R_s i_s) dt \quad (6)$$

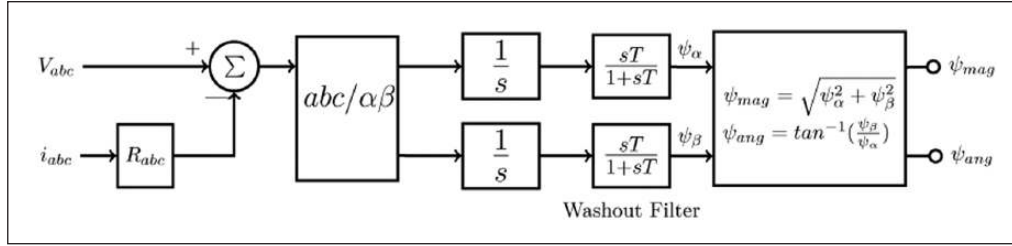


Figure 2. Rotor flux magnitude and angle calculation.

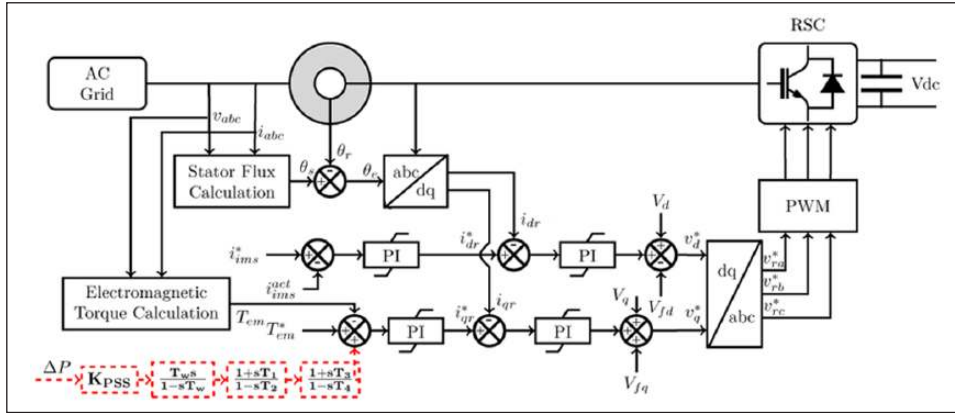


Figure 3. Rotor side converter (RSC) control.

$$\psi_{mag} = \sqrt{\psi_{\alpha}^2 + \psi_{\beta}^2} \quad (7)$$

$$\psi_{ang} = \tan^{-1}\left(\frac{\psi_{\beta}}{\psi_{\alpha}}\right) \quad (8)$$

The magnitude and angle of magnetic flux are calculated as shown in Figure 2. The washout filter is used to extract the 50 Hz component of the flux in $\alpha - \beta$ frame. The control scheme of the RSC is as shown in Figure 3.

The speed error and magnetizing current error are fed to the proportional–integral (PI) controllers which gives the reference dq currents (i_{dr}^* and i_{qr}^*). The inner current loop is employed to find the voltage references. The reference voltages are transformed back to “abc” frame with a transformation angle θ . As the rotor injected currents are in slip frequency, the θ is found out as

$$\theta = \psi_{ang} - \theta_e \quad (9)$$

where θ_e is the rotor angle position, which can be calculated as, $\theta_e = \int(\omega_e)dt$

The switching pulses are generated such a way as to track the converter voltages to the reference voltages in “abc” frame with the converter gain. Sinusoidal PWM method is used to generate the switching pulses with a switching frequency of 10 kHz.

GSC control

The DC link voltage is affected by the amount of active power flowing through the converter and switching losses in the converters. The RSC control get disturbed when the DC link voltage changes. Therefore, primary objective of GSC is to

maintain the DC link at 1 p.u. during the entire operation of DFIG (including sub synchronous and super synchronous modes).

The voltage balance equations at the GSC terminals can be written as

$$\begin{bmatrix} v_a \\ v_b \\ v_c \end{bmatrix} = R \begin{bmatrix} i_a \\ i_b \\ i_c \end{bmatrix} + L \frac{d}{dt} \begin{bmatrix} i_a \\ i_b \\ i_c \end{bmatrix} + \begin{bmatrix} v_{ag} \\ v_{bg} \\ v_{cg} \end{bmatrix} \quad (10)$$

where, v_a, v_b, v_c are the converter output voltage, i_a, i_b, i_c are the currents from converter to grid; v_{ag}, v_{bg}, v_{cg} are the grid voltages; and R, L are the resistance and inductance, respectively, in converter to grid path, (including the transformer leakage reactance).

The three phase active and reactive power can be expressed in dq frame as

$$p = v_d i_{ds} + v_q i_{qs} \quad (11)$$

$$q = v_q i_{ds} - v_d i_{qs} \quad (12)$$

For GSC, d axis is aligned with the stator voltage

$$v_d = V \text{ and } v_q = 0 \quad (13)$$

The active and reactive power expression can be reduced to

$$p = v_d i_{ds} \text{ and } q = -v_d i_{qs} \quad (14)$$

Therefore, i_{ds} is proportional to active power flow and i_{qs} is proportional to reactive power flow through the GSC.

As shown in equation (14), the active power flow through GSC is directly proportional to direct axis converter current i_{ds} . In order to compensate the active power loss in the converter (switching loss) and capacitor loss (due to parasitic resistance), the active power through the converter is controlled by regulating i_{ds} . Similarly reactive power flow through the converter is controlled by i_{qs} . The control scheme of GSC is as shown in Figure 4.

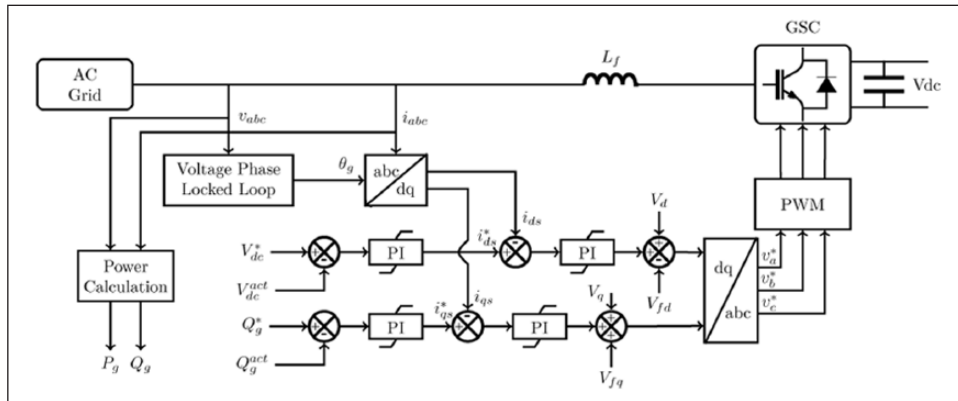


Figure 4. Grid side converter (GSC) control.

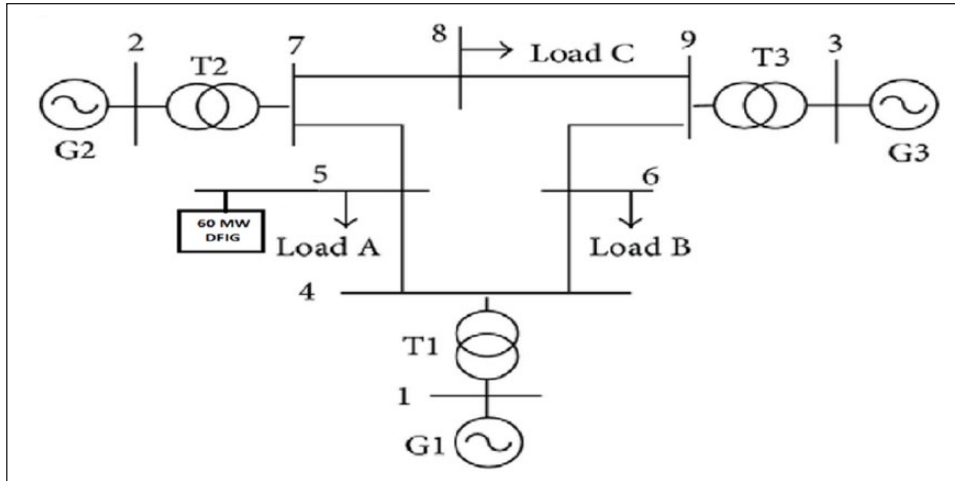


Figure 5. WSCC system.

The DC link voltage error and reactive power error are fed to the PI controllers which produce the respective controlling variables, i_{ds}^* and i_{qs}^* . The switching pulses are generated such a way as to track the converter currents to the reference currents in “abc” frame. Hysteresis current control method is used to generate the switching pulses. Hysteresis band is selected in such a way that it is small enough to get accurate tracking and high enough to control the switching frequency. The GSC is capable of providing any desired amount of reactive power to the grid depending on the power rating of the converter.

Modeling of power system

The standard 9 bus 3 generator, WSCC system is selected for detailed modeling in PSCAD/EMTDC. The single line diagram of the system is given in Figure 5. The system consists of three synchronous generators, three loads and 6 transmission lines as shown in the figure. All the generators are modeled with its excitation controls, turbine governor control and with PSS. All the transmission lines are modeled as long Bergeron lines which can reflect the transient performance.

The bus 1 is considered as swing bus for voltage angle reference. The excitation system is modeled as IEEE standard “AC8B” model (IEEE Committee, 2006). The turbine governor system is modeled as (IEEE Committee, 1991) to maintain the speed at synchronous speed (Kundur, 1994). To investigate the performance of DFIG in power oscillation damping, a 60 MW wind farm is connected at bus 5. The wind farm is represented by aggregated system of 60 MVA, which actually consists of 30 2 MW DFIG system connected in parallel modeled as equivalent single DFIG driven by single wind turbine (Qiao et al., 2006).

To analyze the power oscillations in the system, the most severe three-phase fault is applied at the different buses in the system. The frequency of power oscillations due to the advancement of rotor angle of synchronous generators after the fault depends on the fault locations and power coefficient of each machine. These power oscillations are found to be in the frequency range of 0.2–12 Hz. These oscillations persist in the entire power system for a quite long time (Sauer and Pai, 2007) even after the operation of PSS.

Power oscillation control

The key strategy to improve transient limit of a system is to regulate the first swing of the rotor angle of the synchronous machine (Kundur et al., 1989). The accelerating power due to the mismatch of mechanical power input and electrical power output during disturbance causes the rotor angle to accelerate and thus causing the power oscillation. The PSS employed at the synchronous machines will try to damp the oscillation by changing the terminal voltage of the synchronous machine dynamically with the change in the rotor speed. Advantage of power electronics-based reactive power control over conventional methods is that it can alter the $P-\delta$ curve very fast by regulating the reactive power flow during the power oscillation (Molinas et al., 2008).

In order to counteract the accelerating and decelerating swings of the disturbed machines, it is necessary to vary the active and reactive power supplied at the terminals of the DFIG terminals. That is the reactive power supply from the

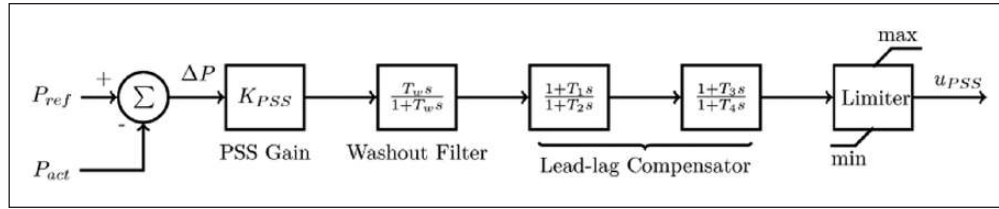


Figure 6. Classical power system stabilizer.

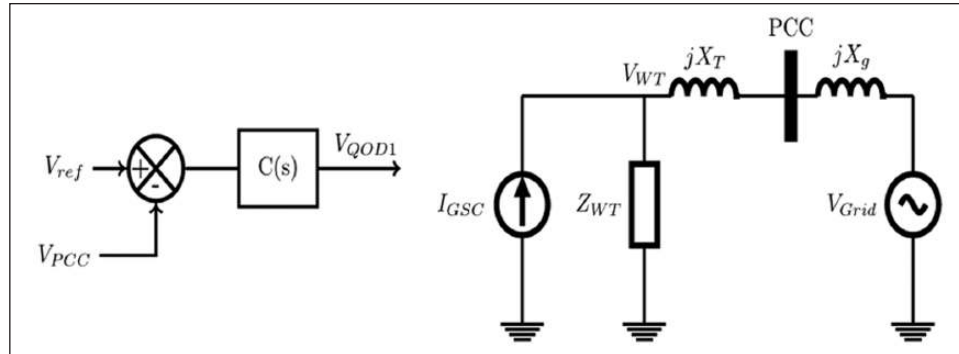


Figure 7. Simplified circuit of DFIG for reactive power modulation.

GSC should be capable of increasing the electric power transmitted during rotor angle acceleration (when $\frac{d\delta}{dt} > 0$) and decreasing the electric power during rotor angle deceleration (when $\frac{d\delta}{dt} < 0$).

The RSC of DFIG is protected using crowbar resistances during fault to limit the RSC current within the allowed limits (Morren and de Haan, 2005). Due to the FRT capability, the DFIG system remains connected to the grid after clearing the fault following the grid code and can take part in the reactive power regulation. The active power flow in the system start oscillates according with the rotor angle dynamics. The reactive power injection from GSC can alter the voltage of the bus to which it is connected by “bang-bang” theory (Nguyen-Duc et al., 2010). The reactive power injection from DFIG is forcefully made to its max/min limits depending on the rotor angle dynamics whether it is in accelerating/decelerating area in $P-\delta$ curve. The following controllers are employed for DFIG system to damp out the power oscillations.

Auxiliary damping controller

The main objective of auxiliary controller is to make sure that no new oscillation modes are introduced by DFIG to the system. Therefore, PSS for DFIG should be capable to damp the low-frequency oscillations in the range of 0.1–2 Hz, which are known as inter area or local modes (Edrah et al., 2015). The control signal to the PSS can be chosen from any of the oscillation affected parameter like frequency, rotor speed, voltage, power order, and so on.

The location and parameter to be sensed depends on the communication system available in the network and the parameter which can reflect the mode of oscillation (Yohanandhan and Srinivasan, 2016). The point of common coupling (PCC) of the wind farm is selected to reduce the filtering effects and minimize the communication requirements. The conventional PSS with lead—lag compensator can be represented by Figure 6.

Any feedback signal which has sufficient modal observability of oscillations can be used as the input for PSS. The active power flow through the lines, voltage angle differences, generator rotor angle differences etc are commonly used signals. Since the DFIG system may not be synchronously connected to the system, rotor angle and frequency may not be good feedback signals for PSS (Mendonca and Lopes, 2009). The active power output of DFIG can be used as input, as the wind speed can be assumed to be constant during the small time period of oscillation. The washout filter and lead lag compensator extracts the specific mode of oscillation and provides the control variable for damping. The PSS can take only the signals which are measured from the PCC which can reflect only the local mode of oscillation (Shahgholian and Movahedi, 2016). The output signal PSS is directly coupled with RSC control for torque regulation.

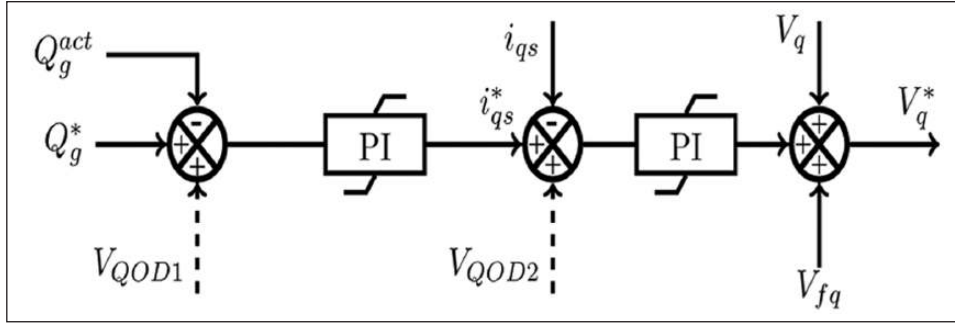


Figure 8. Control diagram of ΔQOD in GSC control.

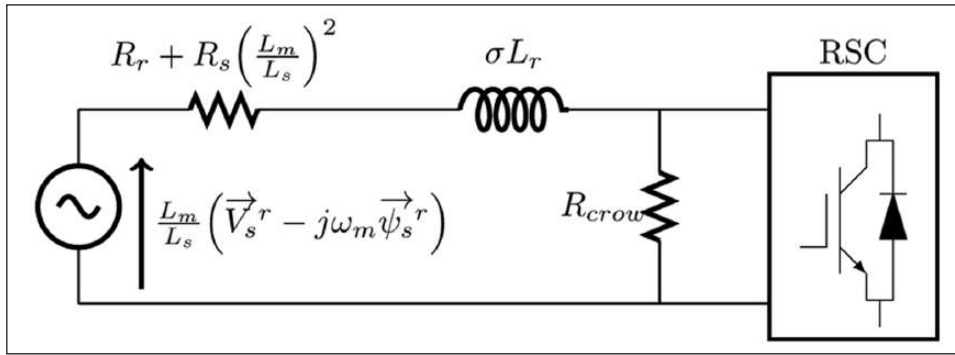


Figure 9. Equivalent circuit of DFIG system with crowbar.

Reactive power control

The power oscillations that occur in the power system after clearing the fault can be damped out by modulation of DFIG reactive power output by providing a certain phase shift with respect to the input signal that contains oscillation. The torsional interactions of mechanical turbines which may cause resonance limits the frequency range of DFIG operations in power oscillation damping (Fan et al., 2011). To achieve a positive damping, the output reactive power from DFIG has to be tightly controlled. The ability of DFIG to damp the oscillation depends on (1) interaction of ΔQ power oscillation damping (POD) and the PCC voltage and power factor, (2) speed of controller action to track the phase shift in the reactive power, and (3) strength of the grid. To evaluate the proposed ΔQ POD method, fault is applied at different buses (to get variable operating conditions for DFIG) and presented in the section “Simulation Results.”

The PCC voltage is altered to change the reactive power output of DFIG by controlling the reactive power component of the current from GSC as shown in Figure 4. To illustrate control loop, a simplified circuit as shown in Figure 7 is considered.

The performance of the controller to track the reference voltage is analyzed using the transfer function defined between the DFIG terminal voltage and the infinite bus

$$\begin{aligned} V_{QOD} &= T_1(s)V_{ref} + T_2(s)V_{Grid} \\ &= \frac{C(s)}{\frac{1}{X_T + X_g} + \frac{X_{WT}}{|Z_n|^2} + C(s)} V_{ref} \end{aligned} \quad (15)$$

$$+ \frac{1}{(X_T + X_g)(C(s) + \frac{X_{WT}}{|Z_n|^2}) + 1} V_{Grid} \quad (16)$$

For ideal cases, $T_1(s) = 1$ shows the perfect tracking of the voltage. From the expression of $T_2(s)$, it is possible to investigate the factors effecting the voltage tracking ability. For common WECS installation, $X_g \gg X_T$ and as the short circuit

ratio (SCR) increases, that is, X_g decreases, the ability to track the reference reduces. Therefore, $\Delta QPOD$ method can significantly support for the voltage and damp out the oscillations if the fault is at the farther end from DFIG. The ΔQOD controller output is added to the outer loop of the GSC in order to modulate the reactive power by giving the specific phase shift to the voltage output.

The ΔQOD method is employed with two input variables for the controllers' reference values, viz. (1) V_{QOD1} and (2) V_{QOD2} . The V_{QOD1} input variable corresponds to the tracking of the desired phase shifted voltage, and V_{QOD2} corresponds to the rejection of disturbance occurring in the oscillation information. The general structure of ΔQOD is as shown in Figure 8. As the frequency of oscillation increases, the phase shift provided by the ΔQOD will be more phase lagged. For a typical SCR > 10, the phase lag provided by the ΔQOD will be $\pm 15^\circ$. The low frequencies of oscillations are canceled out by the fast controller action of GSC which can provide large phase shift with low gain.

Coordinated control with crowbar resistance

The crowbar resistance is normally disconnected from rotor side, once the fault is cleared from the system. The RSC current is highly influenced by the crowbar connection and hence can affect the amount of power delivered from the rotor side (Cheng and Cai, 2011). Therefore, the power oscillation can be controlled by fast switching of the crowbar just after clearing the fault. The crowbar resistance is connected to the rotor through a controlled bridge and thus the power dissipated can be controlled.

The crowbar resistance is connected to the rotor through a three-phase fully controlled converter. Therefore, the power dissipation in the crowbar can be controlled by controlling the switching pulses to the converter. To limit the current through the converter, additional reactance is included in addition to the rotor reactance.

Crowbar topology

When crowbar is activated, the rotor side circuit acts as an impedance divider: RSC voltage is a fraction of the emf induced in the rotor windings. In other words, when crowbar is activated, a circulating current starts developing in the rotor terminals through crowbar, causing a voltage drop in the rotor circuit, which reduces the voltage at the RSC terminals. By regulating the current flow through crowbar, RSC power output can be controlled.

Earlier type of crowbar used diodes or thyristor types bridges, where turn on and turn off cannot be controlled. Modern crowbar uses fully controlled switches like gate turn-off thyristors (GTOs), IGBTs, and so on, where the crowbar resistances can be actively controlled by using Pulse Width Modulation techniques. The switching can be controlled in a way so as to produce a negative resistance also (Mohan and Undeland, 2007). Depending on the power oscillation magnitude, the values of crowbar resistance can dynamically controlled by proper switching control.

Design of active crowbar. The value of crowbar resistance should be chosen carefully so that it should not be too less where the high current might damage the crowbar, and it should not be very high where desired low voltage at RSC terminals is not produced.

- If a very low value is chosen, the short-circuit current will be very large. The crowbar switch should then be oversized and, as will be seen, the electromagnetic torque will have a big peak.
- The rotor current can be reduced by using a higher resistance. However, if the resistance is too big, the crowbar would not pull the rotor voltage low enough. In this case, the rotor current will circulate across the rotor converter via its freewheeling diodes even if it is inactive.

In order to properly protect the rotor converter, the voltage should be kept below the following value

$$V_r = \frac{V_{DC}}{\sqrt{3}} u \quad (17)$$

where V_r is the peak rotor voltage, V_{DC} is the DC link voltage, and n is the turns ratio.

Depending on the PCC voltage and power from DFIG, the natural flux has a direct effect on crowbar dissipated power. The crowbar assists the demagnetizing of the machine and this effect is accentuated when, as is usual, its resistance is low (Haidar et al., 2017).

Control of active crowbar. The equivalent circuit of DFIG system with crowbar is as shown in Figure 9. As mentioned earlier, the crowbar act as a impedance divider which can directly control the RSC terminal voltage by regulating the value of R_{crow} . The voltage balance equation can be written as

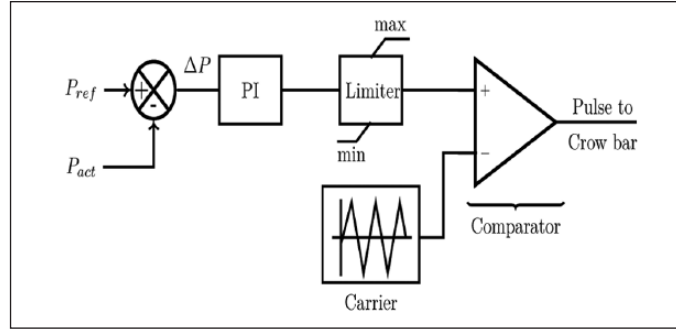


Figure 10. Crow bar control.

$$\bar{V}_r = \frac{L_m}{L_s} (\bar{V}_s^r - j\omega_m \bar{\psi}_s^r) = \bar{i}_r \left(R_r + R_s \left(\frac{L_m}{L_s} \right)^2 + j\sigma L_r \right) \quad (18)$$

The voltage at the RSC terminal can be controlled by regulating the current flowing through crowbar. The power dissipated in the crowbar resistance can be formulated as (Mohan and Undeland, 2007)

$$P_{Crow} = \frac{V_{rotor}^2}{R} \left(1 + \frac{3\sqrt{3}}{4\pi} \cos(2\alpha) \right) \quad (19)$$

The power dissipation in the crowbar is regulated in coordination with the reactive power control from GSC. The crowbar control is activated to regulate the power flowing to the DC link just after clearing the fault by controlling the current to the crowbar resistance. Pulse width modulation technique is employed for generating the switching sequence for crowbar converter. The crowbar control is shown in Figure 10.

It is assumed that the wind speed is constant during the small time period of crowbar operation. The reference power and actual power output of DFIG are compared to calculate the power oscillation and it is fed to PI controller. To regulate the switching and to control the switching frequency, the signal is compared with the carrier signal of constant frequency to generate the gating pulse to the crowbar converter.

Co-ordinated control for power oscillation damping. The combined co-ordinated power oscillation damping can be shown in following operational sequence.

1. Immediately upon the detection of fault, crowbar is activated which demagnetizes the machine.
2. During fault, the excess power from wind is dissipated in the crowbar which regulates the rotor speed and dc link voltage and protect the converters from over currents.
3. Once the fault is cleared, the excited voltages of the generators create oscillations in the system. Depending on oscillation, PSS in rotor circuit of DFIG acts for damping specific mode of oscillations.
4. Once the dc link voltage is settled down after transients, GSC will provide the reactive power support in accordance with the power oscillation as shown in Figure 8.
5. DFIG crowbar converter is activated simultaneously in such a way that, the active power output is regulated by controlling the power dissipated in crowbar using equation (12) and the schema shown in Figure 10.

Thus, the crowbar control regulates the power dissipation at the resistance just after clearing the fault. Since the error signal given to the PI controller is same as that of the reactive power control (Figure 6), both the controllers are coordinated together. During the time of oscillation, all the three controllers (PSS control, ΔQOD control and crowbar control) act in coordination. The PSS will try to damp out the local mode of oscillation in the system, while GSC control tries to improve the voltage at PCC by injecting reactive power and the crowbar control dissipates the extra energy in resistor dynamically. The following section validates the coordinated control over simple PSS operation.

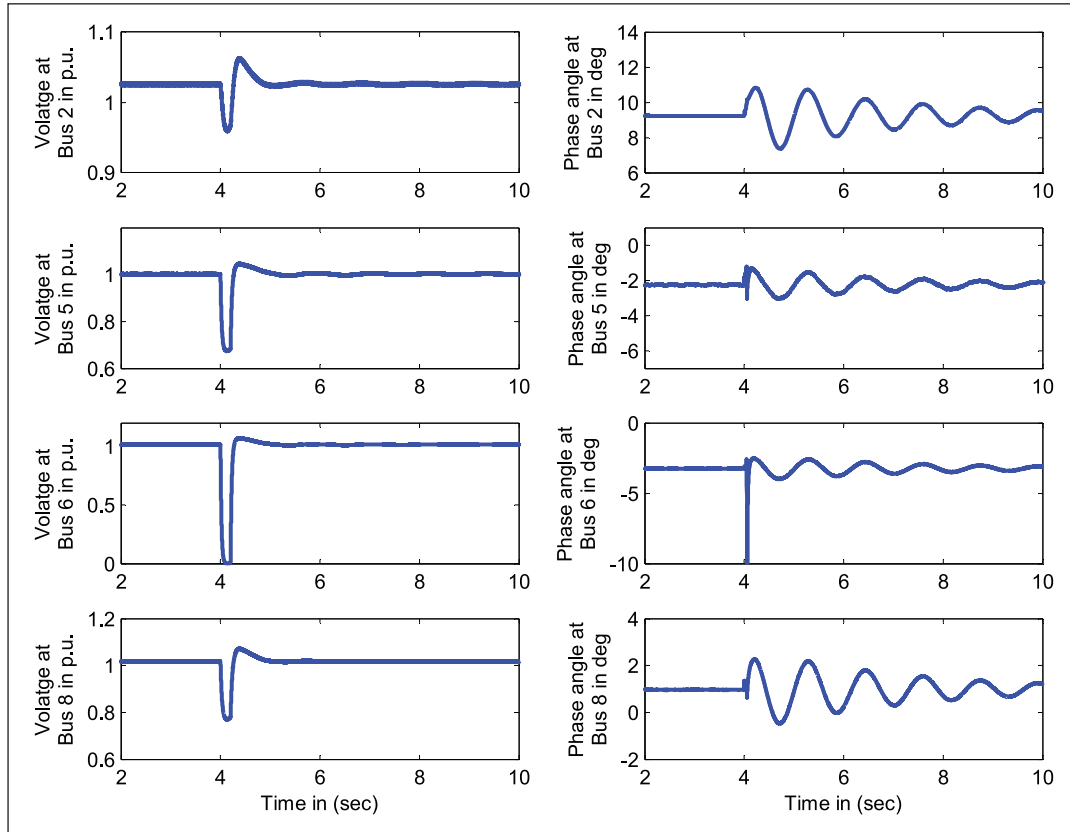


Figure 11. Voltage magnitude and phase angle variation when a three phase fault occurs at bus 6 (case A).

Simulation results

The WSCC 9 bus system is modeled with all the synchronous generator dynamics in PSCAD/EMTDC as discussed earlier. A 60 MW DFIG is connected at bus 5. The mechanical torque input to the DFIG is 0.7 p.u. All the generators are modeled with all its auxiliary controls like excitation control and turbine control. Three different cases are simulated to show the effect of power oscillation damping by DFIG system.

- *Case A.* Base case with conventional synchronous generators and DFIG operating in fixed power factor (in this paper unity pf);
- *Case B.* Power oscillation damping by the proposed control scheme when a three-phase fault occurs at far end of DFIG (fault at bus 6);
- *Case C.* Three-phase fault at a bus nearer to DFIG system (fault at bus 5).

Case A

A three-phase solid ground fault is applied at bus 6 at a simulation time of 4s. The fault is cleared after 150ms. The variation of voltage magnitude and phase angles of selected buses are as shown in Figure 11. The phase angle oscillation after clearing the fault in turn creates the power oscillation in the lines. These oscillations spread out to the entire power system. The power oscillations in the selected transmission lines are as shown in Figure 12. All the line flows are in p.u. for a common base of 100 MVA.

The mechanical input torque from the wind turbine is assumed to be of a constant value, 0.7 p.u., throughout the dynamic operation of the system. The crowbars are connected at the rotor terminals to limit the rotor current which may damage the RSC during fault condition. This makes it possible for the DFIG system to remain connected to the power system even after clearing the fault, following the grid code. The performance of DFIG, with unity power

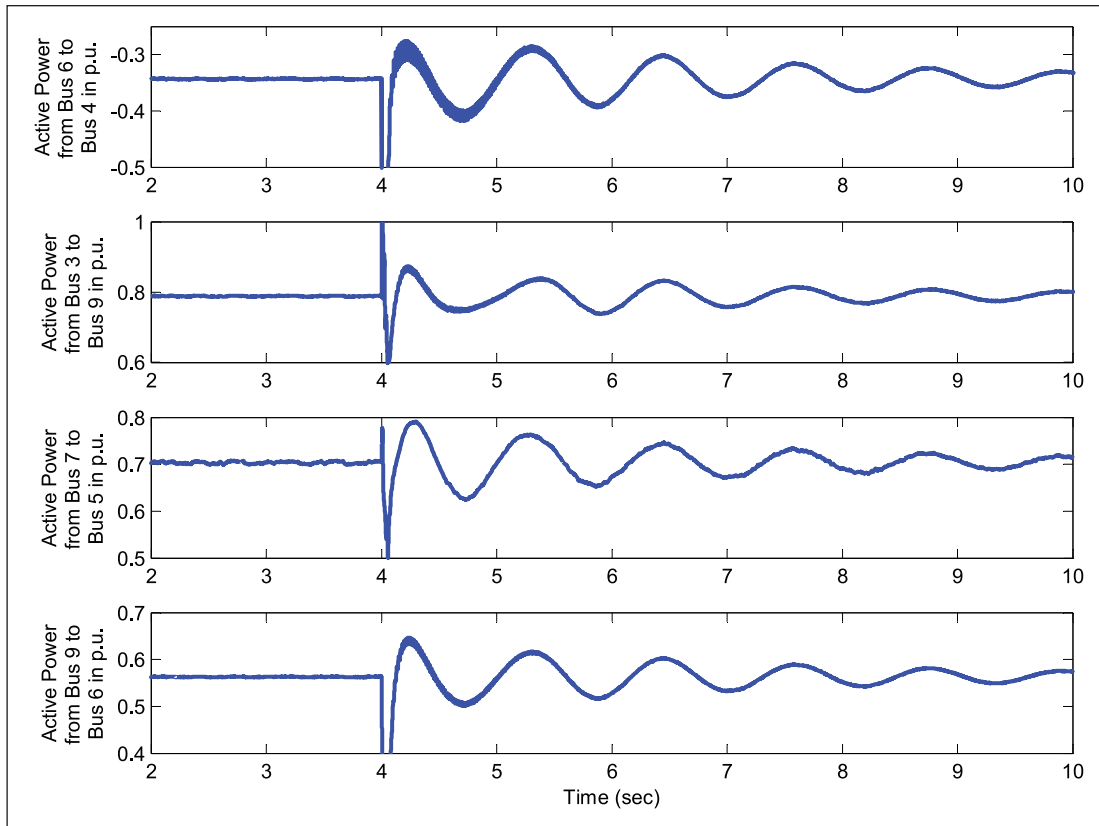


Figure 12. Active power flows in the line when a three phase fault occurs at bus 6 (case A) without DFIG control.

factor operation, the active and reactive power outputs from DFIG to the grid, rotor speed and DC link voltage are shown in Figure 13.

As discussed in 2.1, RSC switching is controlled to maintain the rotor speed at 1 p.u. (The reference rotor speed can be given corresponding to maximum point of wind turbine system (Shen et al., 2009)). As discussed earlier, direct axis GSC current, i_{ds} , controls the DC link voltage and quadrature axis current, i_{qs} , controls the reactive power fed to the grid. The DC link voltage is maintained at 1 p.u., and for unity power factor operation, the reactive power at the DFIG terminals is controlled at 0 MVar. The crowbars are turned ON once the terminal voltage falls below 0.7 p.u. which limits the RSC current and protect the DC link capacitor from over voltage.

The generator bus voltage dynamics are shown in Table 1. The frequency of oscillation in Hertz, damping factor expressed as percentage, natural frequency of oscillation in radians and so on for the two generators are shown. The damping ratio of the two generators is very poor, which causes the power oscillation to remain in the system.

Case B

Three-phase solid fault is applied at bus 6 which is electrically farther from DFIG terminals. The fault is cleared after 150 ms and resuming its original network. The reactive power output of DFIG is controlled as discussed in ΔQOD method. The terminal voltage and power flow of the DFIG are the only available measurements for the control system. The phase lag to the reactive power fed from GSC is provided according to the dynamics of the voltage phase angles.

The rating of the RSC is 30% of the total rating of the machine. Thus, the maximum power (including both active and reactive power) that can be drawn from RSC is 20 MVA. Once the fault is cleared from the system, GSC is controlled to provide phase lagged reactive power to the grid to damp the power oscillations. The active and reactive power outputs from DFIG to the grid, rotor speed and DC link voltage are as shown in Figure 14.

Since the reactive power is supplied from the GSC, the active power injected to the grid from stator side is not much affected due control action. But due to the reactive power compensation from GSC to the line reactances, the DFIG

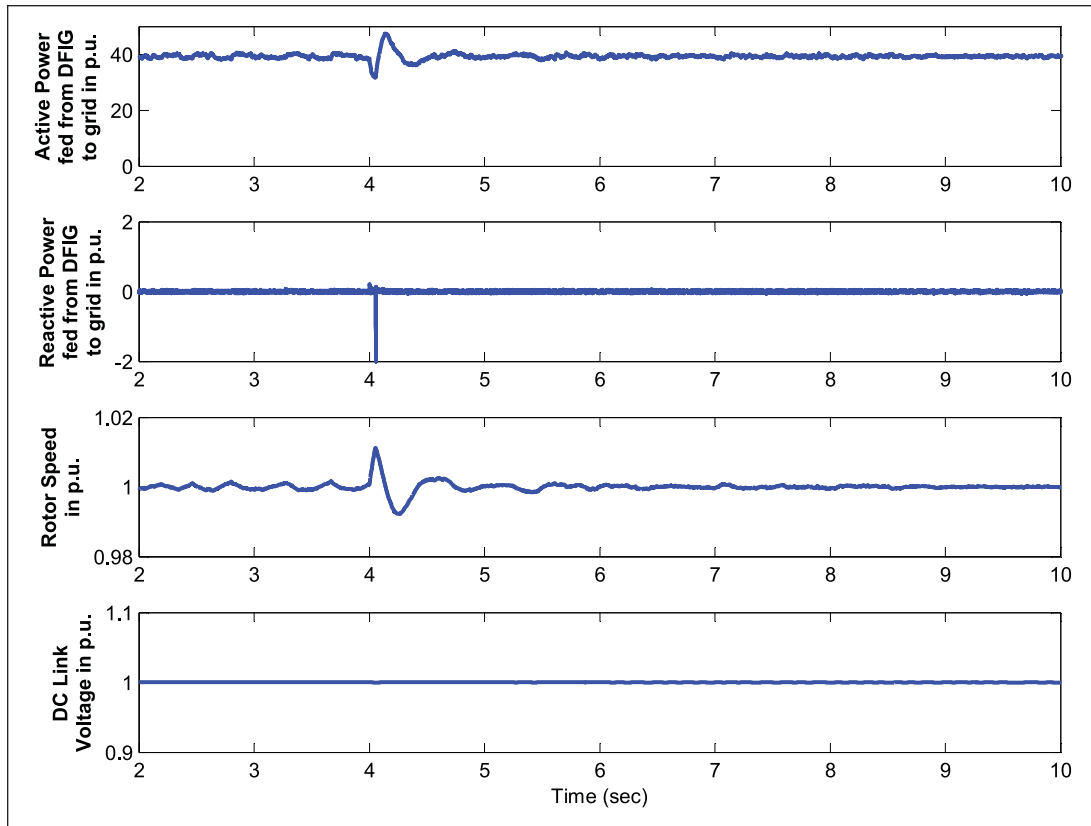


Figure 13. DFIG performance without power oscillation damping control.

Table 1. Generator voltage dynamics.

Parameters	Gen 2	Gen 3
Frequency of oscillation (Hz)	0.8532	0.8826
Damping factor (%)	0.84	0.89
Eigenvalue ($\sigma + j\omega$)	$-0.05 \pm j5.3611$	$-0.0491 \pm j5.5456$
Natural freq. of oscillation (rad)	5.3613	5.5458

terminal voltage is affected and ultimately providing the damping action by regulating the active power flow. The rotor speed is maintained at 1 p.u. and the DC link voltage is also maintained 1 p.u. constant due to the GSC control action.

The synchronous generator terminal voltage dynamics are shown in Figure 15 and corresponding parameters are shown in Table 2. The damping factor of both the generators are improved from earlier case. The damping factor of generator 2 is improved from 0.84% to 1.27% as the transmission line reactance drop is compensated more for generator 3 as the generator 2 is nearer to the DFIG terminals.

The reactive power output of DFIG is regulated, and corresponding line flows are shown in Figure 16. The coordinated reactive power control regulates the voltage magnitudes and effectively damping the power oscillation.

Case C

A three-phase fault occurs at the terminals of the DFIG system. The fault is applied at the terminals of the DFIG at a simulation time of 4 s, and it is cleared after 150 ms and regains its original network. The DFIG speed dynamics is taken for damping control. The reactive power of DFIG is regulated as discussed earlier.

The power flow through the lines with and without control is shown in Figure 17 and the voltage angle oscillation at the two generator buses are shown in Figure 18. DFIG draws a large amount of reactive power from the grid during the

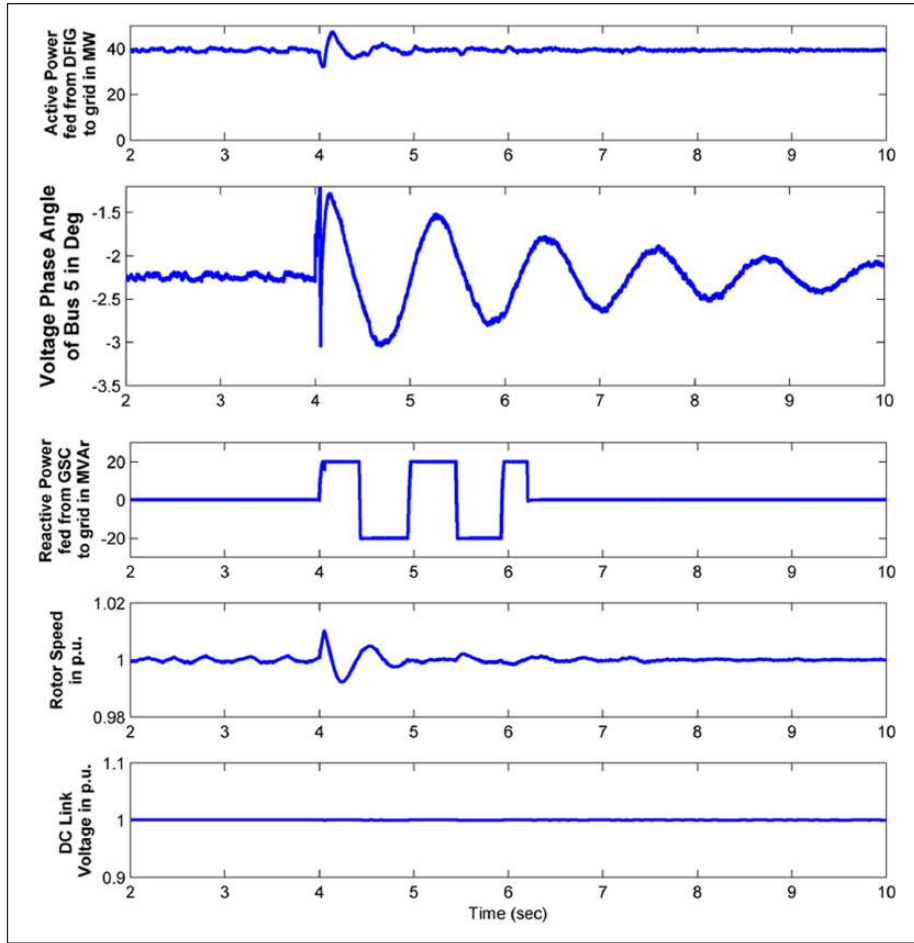


Figure 14. DFIG performance with power oscillation damping control.

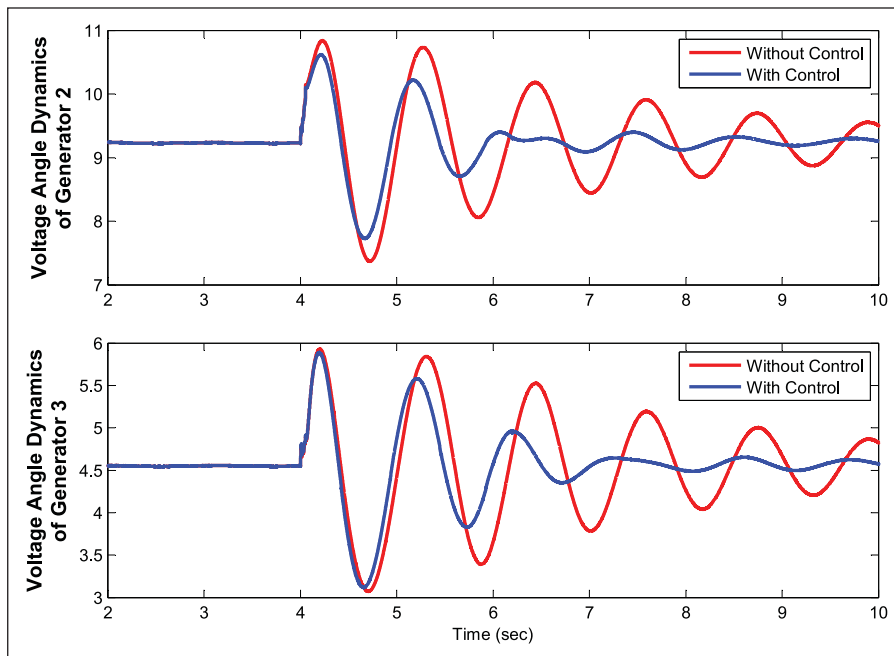


Figure 15. Generator terminal voltage dynamics for a three fault occurs at bus 6 (case B).

Table 2. Generator voltage dynamics (case B).

Parameters	Gen 2	Gen 3
Frequency of oscillation (Hz)	1.1574	1.016
Damping factor (%)	1.25	1.07
Eigenvalue ($\sigma + j\omega$)	$-0.0907 \pm j7.2722$	$-0.0684 \pm j6.38$
Natural freq. of oscillation (rad)	7.2728	6.3857

Table 3. Generator voltage dynamics (case C).

Parameters	Gen 2	Gen 3
Frequency of oscillation (Hz)	1.0526	1.0638
Damping factor (%)	1.54	2.22
Eigenvalue ($\sigma + j\omega$)	$-0.1015 \pm j6.6139$	$-0.1484 \pm j6.6842$
Natural freq. of oscillation (rad)	6.6147	6.6859

fault which reduces the voltage level at all the buses. Once the fault is eliminated, DFIG regains its synchronism and the GSC can provide its maximum reactive power support.

Since the generator 2 is nearer to the fault location, its voltage angle experiences more oscillation. Due to the GSC reactive power control, these oscillations are damped out. The damping ratios experienced by the generators and their eigenvalues are shown in Table 3. This indicates that controlling the reactive power support from GSC of DFIG can improve the transient stability of the overall system.

The power oscillation damping control significantly depends on the location of fault with respect to the DFIG terminals. The simulation results show that if the fault is nearer to the DFIG, the oscillation damping control has less effect, as the reactance between the DFIG terminal and the fault is very small which requires only a less amount of reactive power to improve the voltage profile and thus power flow cannot be modulated accordingly.

The main advantage of this control is it needs only the measurement of power at its terminals which is readily available. It is assumed that the wind torque is constant during the power oscillation damping. The power oscillation damping is done in terms of time for rotor angles to settle down to equilibrium point, rather than changing the frequency of oscillation as WECS cannot change the system parameters during the short fault clearance time.

Conclusion

The low inertia renewable energy integration makes the grid weak and makes it more prone to instability under severe fault conditions. The system voltage goes down during a fault in any part of the power system. If the fault is cleared within the permissible time (based on grid codes), all the elements should be stable and still connected to the system. The rotor angles of synchronous generators accelerate during the fault, and once the fault is cleared, they produce more electric power than required, and thus oscillate at its equilibrium point. The damping action of PSS and other damper circuits try to bring down the rotor angle to equilibrium point. This causes the rotor angle oscillation and thus power oscillation in the system. FRT capability of DFIG and fast controller action makes DFIG-based WECS to actively take part in the power system oscillation damping action possible.

The independent control of reactive power from DFIG is made use for power oscillation damping. Once the fault is cleared from the system, the DFIG tries to modulate the power flow at its terminal bus by controlling the PCC voltage. The DFIG reactive power is regulated (both delivering lagging reactive power and leading reactive power) corresponding to the power oscillation in the system. The main advantage of this control action is that it requires only local measurements like voltage, power flow at the DFIG terminals. Moreover, the power dissipation in the crowbar is also regulated in accordance with the reactive power to damp out the oscillations fast. WSCC system is modeled with WECS connected at one bus with all auxiliary controls in PSCAD/EMTDC. The most severe three-phase fault is simulated at one bus and verified the control action for power oscillation damping. Power oscillation damping depends on the location of fault and amount of reactive power loads and line parameters. The proposed coordinated reactive power control works tight, if there is enough lagging reactive power loads/lines between the DFIG terminal and fault, so that the voltage can be regulated significantly. The growing share of DFIG-based wind

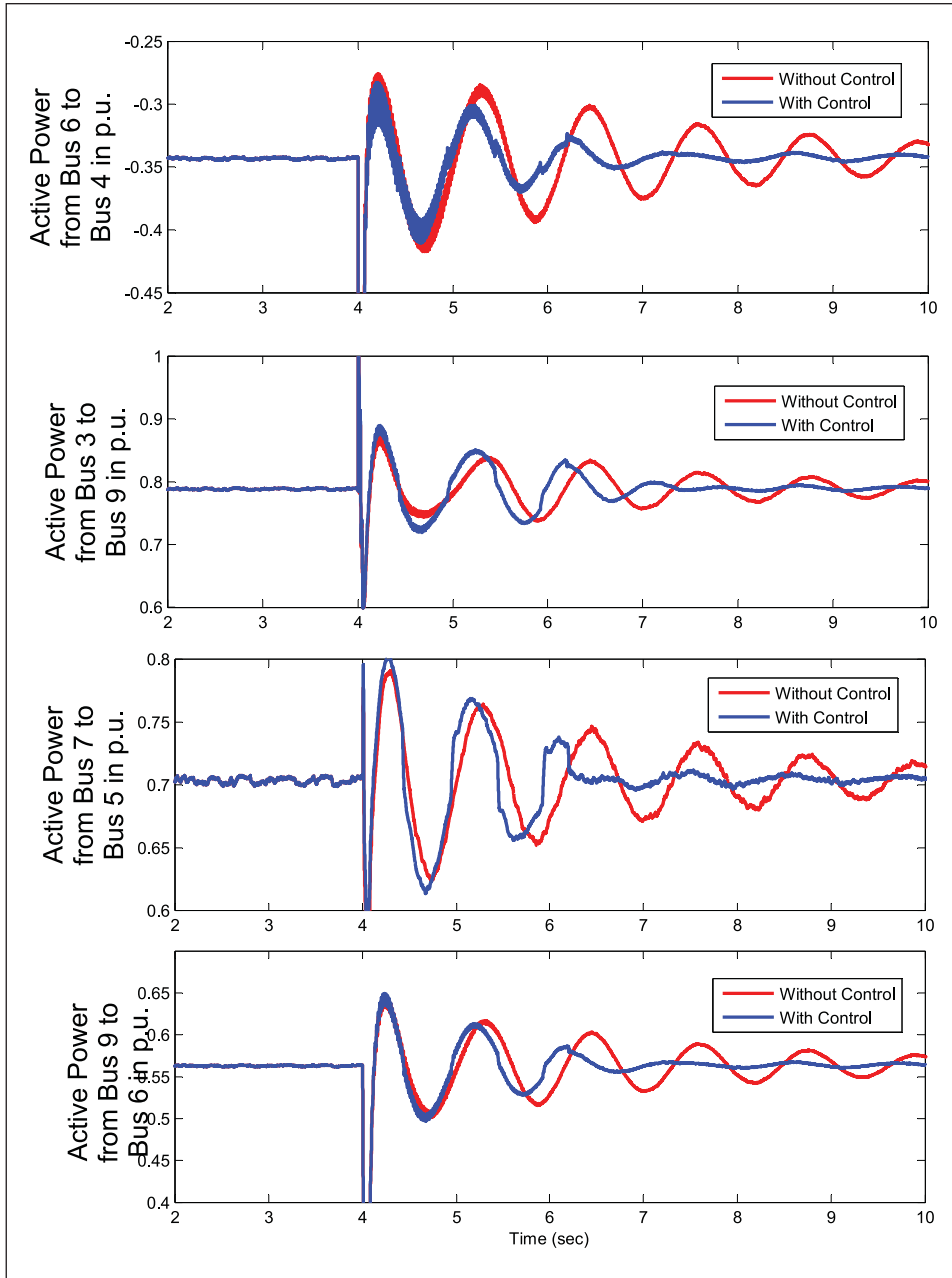


Figure 16. Power flow through lines with and without control for a three phase fault at bus 6 (case B).

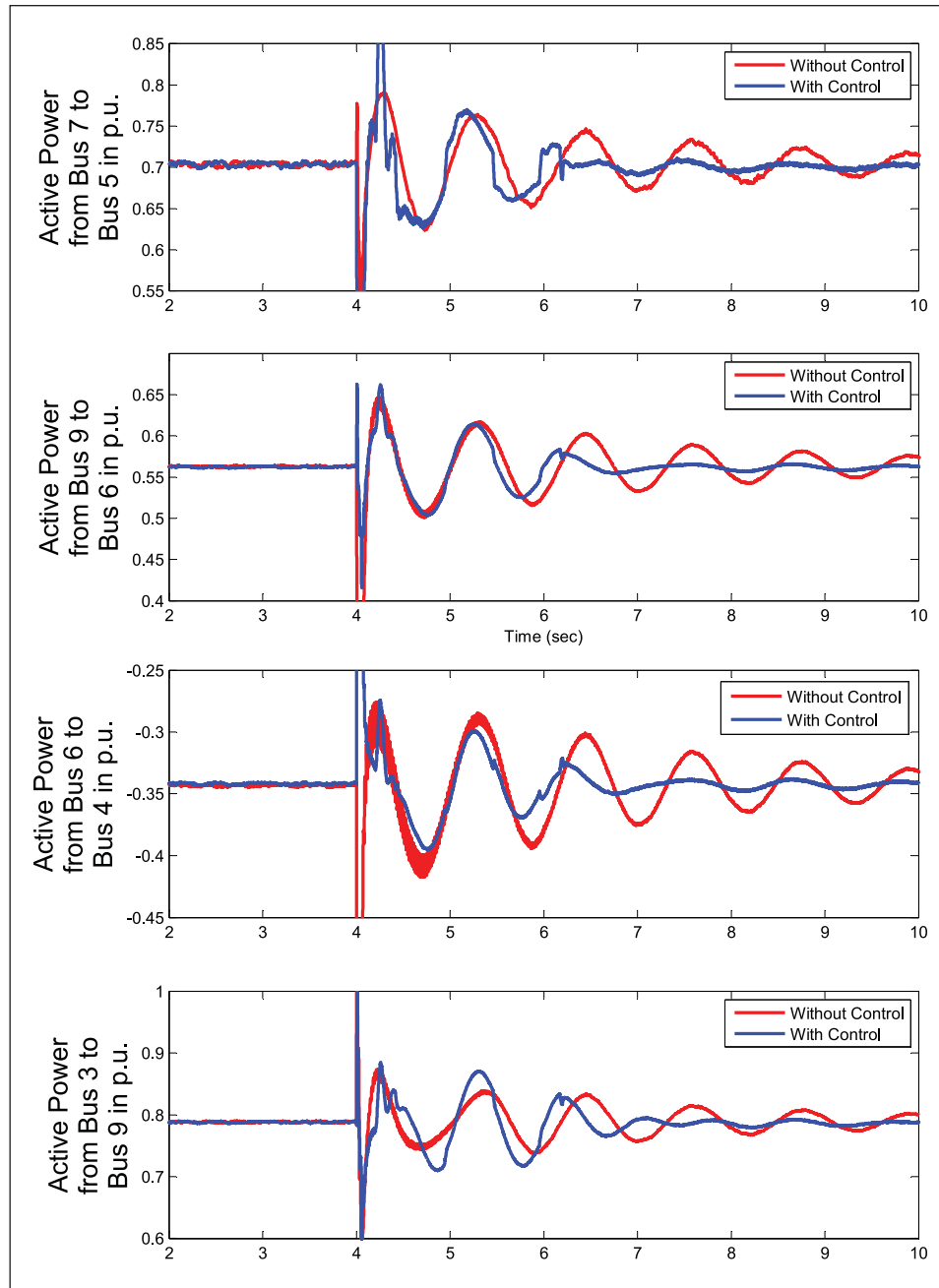


Figure 17. Power flow through lines with and without control for a three phase fault at DFIG terminals (case C).

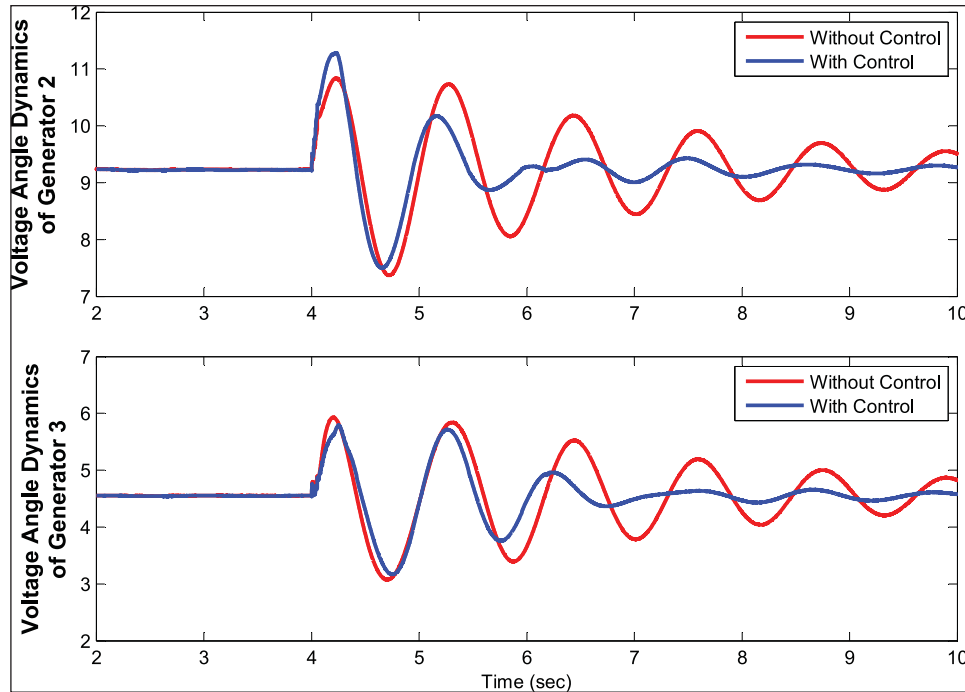


Figure 18. Generator terminal voltage dynamics for a three phase fault occurs at DFIG terminals (case C).

generators with supplementary control actions can improve the system performance significantly and requests vast research activities.

Declaration of conflicting interests

The author(s) declared no potential conflicts of interest with respect to the research, authorship, and/or publication of this article.

Funding

The author(s) received no financial support for the research, authorship, and/or publication of this article.

ORCID iD

Likin Simon  <https://orcid.org/0000-0002-7922-7851>

References

- Akhmatov V (2002) Variable-speed wind turbines with doubly-fed induction generators. *Wind Engineering* 26(2): 85–108.
- Cheng M and Cai X (2011) Reactive power generation and optimization during a power system fault in wind power turbines having a DFIG and crowbar circuit. *Wind Engineering* 35(2): 145–163.
- Datta R and Ranganathan V (1999) Decoupled control of active and reactive power for a grid-connected doubly-fed wound rotor induction machine without position sensors. In: *Industry applications conference (Thirty-Fourth IAS Annual Meeting, Conference Record of the 1999)*, 3–7 October, Phoenix, AZ, vol. 4, pp. 2623–2630. New York: IEEE.
- Edrah M, Lo KL and Anaya-Lara O (2015) Impacts of high penetration of DFIG wind turbines on rotor angle stability of power systems. *IEEE Transactions on Sustainable Energy* 6(3): 759–766.
- Edrah M, Lo KL and Anaya-Lara O (2016) Reactive power control of DFIG wind turbines for power oscillation damping under a wide range of operating conditions. *IET Generation, Transmission Distribution* 10(15): 3777–3785.
- Fan L, Yin H and Miao Z (2011) On active/reactive power modulation of DFIG-based wind generation for interarea oscillation damping. *IEEE Transactions on Energy Conversion* 26(2): 513–521.
- Geng H, Xi X, Liu L, et al. (2017) Hybrid modulated active damping control for DFIG-based wind farm participating in frequency response. *IEEE Transactions on Energy Conversion* 32(3): 1220–1230.
- Gupta AK, Verma K and Niazi KR (2017) Dynamic impact analysis of DFIG-based wind turbine generators on low-frequency oscillations in power system. *IET Generation, Transmission Distribution* 11(18): 4500–4510.

- Haidar AMA, Muttaqi KM and Hagh MT (2017) A coordinated control approach for dc link and rotor crowbars to improve fault ride-through of DFIG-based wind turbine. *IEEE Transactions on Industry Applications* 53(4): 4073–4086.
- Hassan A, Mohamed YS, El-Sawy A, et al. (2011) Control of a wind driven DFIG connected to the grid based on field orientation. *Wind Engineering* 35(2): 127–143.
- Hossain ME (2017). RETRACTED: A new approach for transient stability improvement of a grid-connected doubly fed induction generator-based wind generator. *Wind Engineering* 41(4): 245–259.
- Hughes F, Anaya-Lara O, Jenkins N, et al. (2006) A power system stabilizer for DFIG-based wind generation. *IEEE Transactions on Power Systems* 21(2): 763–772.
- IEEE Committee (1991) Dynamic models for fossil fueled steam units in power system studies. *IEEE Transactions on Power Systems* 6(2): 753–761.
- IEEE Committee (2006). IEEE recommended practice for excitation system models for power system stability studies. *IEEE Std 4215–2005 (Revision of IEEE Std 4215–1992)* (2006): 1–85. DOI:10.1109/IEEESTD.2006.99499.
- Kundur P (1994) *Power System Stability and Control*. New York: McGraw Hill.
- Kundur P, Klein M, Rogers G, et al. (1989) Application of power system stabilizers for enhancement of overall system stability. *IEEE Transactions on Power Systems* 4(2): 614–626.
- Ling Y (2016). The fault ride through technologies for doubly fed induction generator wind turbines. *Wind Engineering* 40(1): 31–49.
- Meegahapola LG, Littler T and Flynn D (2010) Decoupled-DFIG fault ride-through strategy for enhanced stability performance during grid faults. *IEEE Transactions on Sustainable Energy* 1(3): 152–162.
- Mendonca A and Lopes JAP (2009) Robust tuning of power system stabilisers to install in wind energy conversion systems. *IET Renewable Power Generation* 3(4): 465–475.
- Miller T (2010). Theory of the doubly-fed induction machine in the steady state. In: *2010 XIX international conference on electrical machines (ICEM)*, 6–8 September, Rome, pp. 1–6. New York: IEEE.
- Mohan N and Undeland TM (2007) *Power Electronics: Converters, Applications, and Design*. Hoboken, NJ: John Wiley & Sons.
- Molinas M, Suul J and Undeland T (2008) Low voltage ride through of wind farms with cage generators: Statcom versus SVC. *IEEE Transactions on Power Electronics* 23(3): 1104–1117.
- Morren J and de Haan S (2005). Ridethrough of wind turbines with doubly-fed induction generator during a voltage dip. *IEEE Transactions on Energy Conversion* 20(2): 435–441.
- Muljadi E, Butterfield C, Parsons B, et al. (2007) Effect of variable speed wind turbine generator on stability of a weak grid. *IEEE Transactions on Energy Conversion* 22(1): 29–36.
- Muller S, Deicke M and De Doncker R (2002) Doubly fed induction generator systems for wind turbines. *Industry Applications Magazine* 8(3): 26–33.
- Nguyen-Duc H, Dessaint L, Okou A, et al. (2010) A power oscillation damping control scheme based on bang-bang modulation of facts signals. *IEEE Transactions on Power Systems* 25(4): 1918–1927.
- Pena R, Clare J and Asher G (1996) Doubly fed induction generator using back-to-back PWM converters and its application to variable-speed wind-energy generation. *IEE Proceedings on Electric Power Applications* 143(3): 231–241.
- Poller M (2003). Doubly-fed induction machine models for stability assessment of wind farms. In: *2003 IEEE power tech conference proceedings*, 23–26 June, Bologna, vol 3, pp. 6. New York: IEEE.
- Qiao W, Harley R and Venayagamoorthy G (2006) Effects of facts devices on a power system which includes a large wind farm. In: *2006 power systems conference and exposition (PSCE '06)*, 29 October–1 November, Atlanta, GA, pp. 2070–2076. New York: IEEE.
- Rajpurohit BS and Singh SN (2015) Performance analysis of unified doubly-fed induction generator for wind power application. *Wind Engineering* 39(5): 533–548.
- Sauer PW and Pai MA (20047) *Power System Dynamics and Stability*. Champaign, IL: Stipes Publishing.
- Shahgholian G and Movahedi A (2016) Power system stabiliser and flexible alternating current transmission systems controller coordinated design using adaptive velocity update relaxation particle swarm optimisation algorithm in multi-machine power system. *IET Generation, Transmission Distribution* 10(8): 1860–1868.
- Shen B, Mwinyiwiwa B, Zhang Y, et al. (2009) Sensorless maximum power point tracking of wind by DFIG using rotor position phase lock loop (PLL). *IEEE Transactions on Power Electronics* 24(4): 942–951.
- Simon L and Swarup KS (2016) Impact of DFIG based wind energy conversion system on fault studies and power swings. In: *2016 National Power Systems Conference (NPSC)*, 19–21 December, Bhubaneswar, India, pp. 1–6. New York: IEEE.
- Singh M, Allen AJ, Muljadi E, et al. (2015) Interarea oscillation damping controls for wind power plants. *IEEE Transactions on Sustainable Energy* 6(3): 967–975.
- Wang L and Vo QS (2013) Power flow control and stability improvement of connecting an offshore wind farm to a one-machine infinite-bus system using a static synchronous series compensator. *IEEE Transactions on Sustainable Energy* 4(2): 358–369.
- Xu L and Cheng W (1995) Torque and reactive power control of a doubly fed induction machine by position sensorless scheme. *IEEE Transactions on Industry Applications* 31(3): 636–642.
- Yohanandhan RV and Srinivasan L (2016) Decentralised wide-area fractional order damping controller for a large-scale power system. *IET Generation, Transmission Distribution* 10(5): 1164–1178.